

Tunable charge carriers and thermoelectricity of single-crystal $\text{Ba}_8\text{Ga}_{16}\text{Sn}_{30}$

M. A. Avila,¹ D. Huo,^{1,2} T. Sakata,¹ K. Suekuni,¹ and T. Takabatake¹

¹Department of Quantum Matter, ADSM, Hiroshima University, Higashi-Hiroshima 739-8530, Japan

²College of Materials Science and Engineering, Donghua University, Shanghai 200051, China

(Dated: February 8, 2020)

We have grown single crystals of the type-VIII intermetallic clathrate $\text{Ba}_8\text{Ga}_{16}\text{Sn}_{30}$ from both Sn and Ga flux, evaluated the stoichiometries through electron microprobe analysis and studied their transport properties through measurements on temperature dependent resistivity, thermopower and Hall coefficient. Crystals grown in Sn flux show n-type carriers and those from Ga flux show p-type carriers, whereas all measured stoichiometries remain very close to the nominal 8:16:30 proportion of Ba:Ga:Sn, expected from charge-balance principles. Our results indicate a very high sensitivity of the charge carrier nature and density with respect to the growth conditions, leading to relevant differences in transport properties which point to the possibility of tuning this material for improved thermoelectric performance.

I. INTRODUCTION

Research on intermetallic clathrate compounds with general formula $\text{A}_8\text{X}'_{16}\text{X}_{30}$ ($\text{A} = \text{Ba}, \text{Sr}, \text{Eu}$; $\text{X}' = \text{Al}, \text{Ga}, \text{In}$; $\text{X} = \text{Si}, \text{Ge}, \text{Sn}$) has increased significantly over the past 10 years, since the proposal that the generic class of caged compounds with guest atoms might be good candidates to fulfill the phonon-glass electron-crystal (PGEC) concept of a thermoelectric material with potential for applications.¹ The cages in these clathrates are formed by $\text{X}'\text{X}$ host atoms connected through diamond-like hybridized orbitals, while the A guest atom lies within the cage and donates two electrons to it. For each divalent A ion in this particular family, the replacement of two X atoms with X' ions in the cage appears to be the required charge-balance condition for these two electrons to be accepted and for the structure to be stabilized.

The potential phonon-glass behavior results from the fact that the A^{2+} ion can in certain cases be loosely bound inside a cage that is slightly oversized in comparison with its ionic radius, and is thus able to achieve a rather independent “rattling” motion that tends to scatter low-frequency acoustic phonons, responsible for a good fraction of the heat conduction in a crystalline lattice.² In the case of $\text{Sr}_8\text{Ga}_{16}\text{Ge}_{30}$ and $\text{Eu}_8\text{Ga}_{16}\text{Ge}_{30}$, the additional presence of a four-fold splitting of an A atom site and the consequent tunnelling of this ion between these four off-center sites is claimed to be the source of truly glass-like behavior in their thermal conductivities at low temperatures.^{3,4,5,6} The electron-crystal characteristic of these clathrates is preserved because the charge carriers remain within the cage network and are not significantly affected by the rattling motion of the guest atom.

We have recently reported a thorough characterization of the basic physical properties of the Type-VIII clathrate $\text{Ba}_8\text{Ga}_{16}\text{Sn}_{30}$, grown as large single crystals out of Sn flux.⁷ Electron probe microanalysis (EPMA) showed that these crystals grew with stoichiometry very close to 8:16:30 despite the excess Sn flux, confirming the relevance of the above mentioned charge balance in

the stabilization of the structure. These crystals showed behavior consistent with a heavily-doped *n*-type semiconductor with large negative thermopower and negative Hall coefficient. They also showed low lattice thermal conductivity of order 1 W/m K resultant from the rattling of Ba ions, which was evidenced by large isotropic displacement parameters in single crystal x-ray diffraction analysis and the presence of Einstein vibrational degrees of freedom in heat capacity analysis.

Towards the end of the experimental investigations for that work, we also succeeded in growing single crystalline $\text{Ba}_8\text{Ga}_{16}\text{Sn}_{30}$ out of Ga flux, and EPMA analysis once again showed a crystal stoichiometry very close to 8:16:30. Since these Ga-flux crystals did not grow as easily or as large as the Sn-flux ones, and the final stoichiometry was not significantly changed, they were not investigated in detail for that initial characterization. However, a recent study of sintered samples of $\text{Ba}_8\text{Ga}_{16+x}\text{Sn}_{30-x}$ (x is the nominal composition) showed that the carrier changes from electron-type for $x \leq -2$ to hole-type for $x \geq -1$.⁸ This result invited a more careful investigation on the dependence of our crystal’s properties with their growth conditions.

In the present work, we extend and complete the basic characterization of single crystalline $\text{Ba}_8\text{Ga}_{16}\text{Sn}_{30}$ with a comparative study between Sn-flux and Ga-flux grown crystals. We will show that the transport properties are in fact highly sensitive to stoichiometry and/or growth conditions, and thus this material has a potential *tunability* that may in principle allow significant improvements in terms of its thermoelectric performance.

II. EXPERIMENTAL DETAILS

Four single crystal batches were prepared and measured for this work: two using excess Sn flux and two using excess Ga flux. Samples from these batches will be referred to as Sn#1, Sn#2, Ga#1 and Ga#2 respectively. Sn#1 samples are from the same crystal growth described in detail in the previous work⁷ using a Ba:Ga:Sn starting proportion of 8:16:60, and Sn#2 samples are from a

TABLE I: Relative Ba:Ga:Sn content in the four measured crystals as determined by electron-probe microanalysis, and Fermi energies derived from thermopower analysis.

Batch Name	Starting Composition	Crystal Stoichiometry			E_F (meV)
		Ba	Ga	Sn	
Sn#1	8:16:60	8.0	16.0	30.0	88
Sn#2	8:16:60	8.1	15.9	30.1	175
Ga#1	8:38:30	8.1	16.1	29.9	225
Ga#2	8:26:30	7.9	16.3	29.7	525

second batch of crystals grown essentially by the same route. With Sn flux the crystals tend to grow very large (limited mostly by the total mass of the starting reagents and by the quartz tube size of order 10 mm in diameter) and have very well defined polyhedral surface facets.

For the Ga#1 and Ga#2 growths the starting elemental proportions were 8:38:30 and 8:26:30 respectively. The high-purity elements were sealed in evacuated quartz tubes, soaked above 1150 °C for 2-3 hours, cooled over 10 hours to 550 °C and then slowly cooled over 100 hours to 420 °C. At this point the ampoules are quickly removed from the furnace and the remaining molten Ga flux separated by centrifuging. Polyhedral crystals grown from this approach were never larger than about 3 mm in diameter. Some of our growth attempts resulted in large plate-like crystals rather than the expected polyhedrons. EPMA analysis showed that these plates are a new compound BaGa₃Sn, which we intend to characterize and describe in a future communication.

To ensure the best possible reliability of a comparative EPMA evaluation of the Sn- and Ga-flux grown Ba₈Ga₁₆Sn₃₀ crystals, we mounted one crystal from each batch on a single sample holder and measured all four in a single experimental session at a JEOL JXA-8200 microanalyzer, using the same reference materials for Ba, Ga and Sn. The results are shown in table I. All crystal stoichiometries remain close to the nominal 8:16:30 proportion, but there are clear distinctions. Sample Sn#1 is, within experimental error, in the ideal stoichiometry. Samples Sn#2 and Ga#1 show a slight excess of Sn and Ga respectively, and sample Ga#2 showed the greatest off-stoichiometry composition (excess Ga).

Electrical resistivity experiments using standard 4-probe geometry were performed on a home-made system in the range of 4-300 K. Thermopower was measured on a home-made system between 4 and 300 K, and on a commercial MMR Technologies system between 300 and 500 K. Hall coefficient experiments were performed on a home-made system between 4 and 300 K, using an applied field of 1 T.

III. EXPERIMENTAL RESULTS

The resistivity behavior $\rho(T)$ below room temperature of all samples is shown in Fig. 1. They are in the

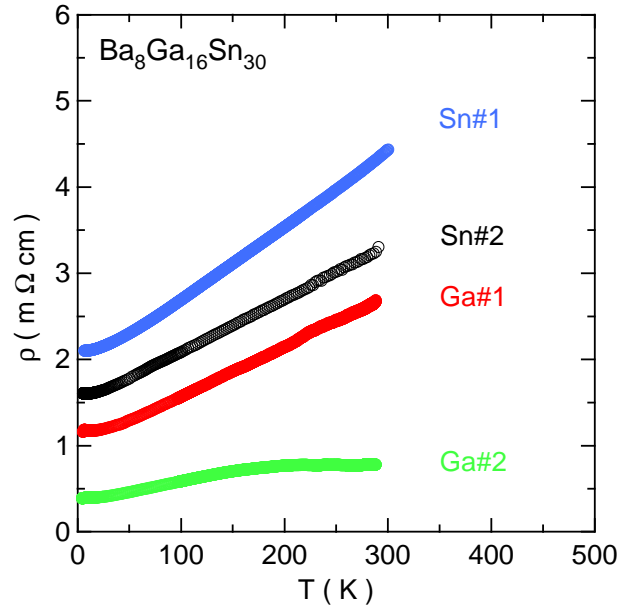


FIG. 1: (color online) Temperature dependence of the electrical resistivity $\rho(T)$ of Ba₈Ga₁₆Sn₃₀ crystals grown from Sn and Ga flux.

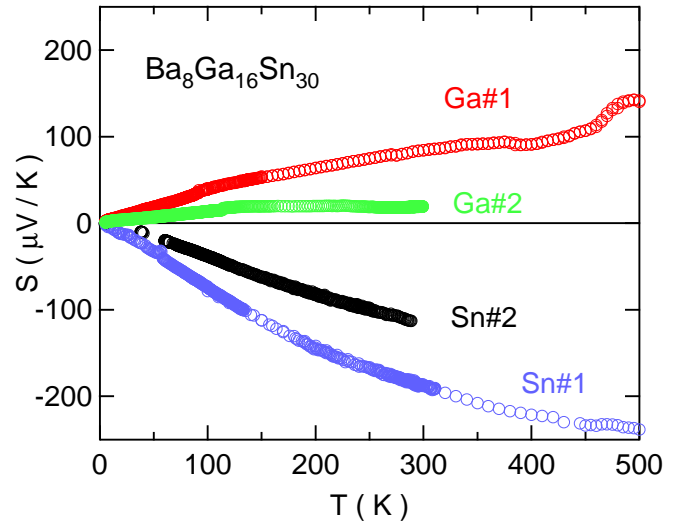


FIG. 2: (color online) Temperature dependence of the thermoelectric power $S(T)$ of Ba₈Ga₁₆Sn₃₀ crystals grown from Sn and Ga flux.

$\text{m}\Omega \text{ cm}$ range and show monotonically decreasing values upon cooling, characteristic of heavily-doped semiconductors or low carrier-density metals. Since these are large, dense and carefully cut samples, (rectangular cross-sections of order $A = 1 \text{ mm}^2$) the uncertainty in estimating the geometrical factor A/d is relatively small (less than 5%), so the differences observed in the calculated resistivities should not be resultant from trivial geometrical uncertainty. The quasi-stoichiometric Sn#1 sample has the highest resistivity, consistent with the idea that the ideal material tends towards a narrow-gap semicon-

ductor. But none of the $\text{Ba}_8\text{Ga}_{16}\text{Sn}_{30}$ crystals grown so far have shown semi-conducting resistivity like that of $\text{Ba}_8\text{Ga}_{16}\text{Ge}_{30}$, so the question remains open whether there is a true gap or a pseudo-gap in the ideal material. The Sn#2 and Ga#1 samples have smaller resistivities, as one would expect from the electron and hole doping effect of their respective non-stoichiometries, and the Ga#2 sample has the lowest resistivity, consistent with its largest doping level.

The differences between the type of charge carriers and its densities become much more evident in the thermopower measurements. In Fig. 2 we show $S(T)$ for the same samples in Fig. 1. As shown in the previous work, Sn#1 sample has negative, monotonically decreasing thermopower in the entire temperature interval (n-type carriers) and reaches a relatively large magnitude of $-185\mu\text{V/K}$ at 290 K. The Sn#2 sample shows somewhat smaller but qualitatively similar behavior, reaching $-113\mu\text{V/K}$ at 290 K. In contrast, the two Ga flux samples show positive $S(T)$ over the entire measured interval, indicating p-type carriers. Sample Ga#1 reaches $+83\mu\text{V/K}$ at 290 K, while sample Ga#1 remains below $+20\mu\text{V/K}$. The best fits of these $S(T)$ curves using a single-band parabolic model⁹ give the Fermi energy values listed in table I.

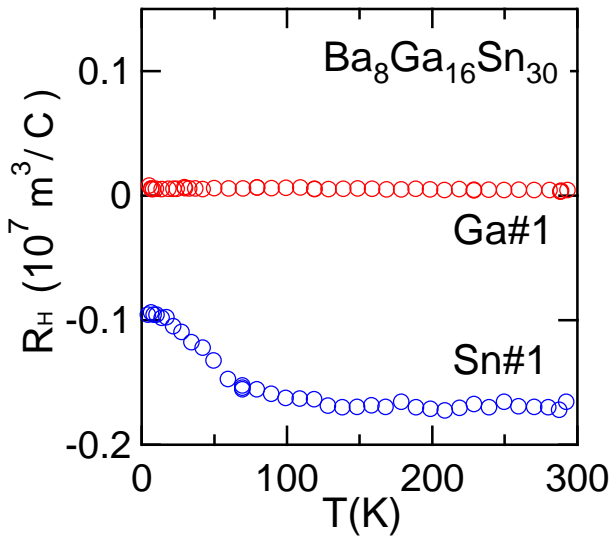


FIG. 3: (color online) Temperature dependence of the Hall coefficient R_H of $\text{Ba}_8\text{Ga}_{16}\text{Sn}_{30}$ crystals grown from Sn and Ga flux.

Further confirmation of these distinctions for different fluxes came with the Hall coefficient measurements, shown in fig. 3. A sample from batch Sn#1 shows negative R_H in the entire temperature interval, while a sample from batch Ga#1 showed a very small and positive R_H . From the single-band model, the carrier concentration $n = 1/eR_H$ obtained from these measurements at 300 K are 3.7×10^{19} electrons/cm³ and 1.3×10^{21} holes/cm³ respectively. The temperature dependence of the Hall mobility $\mu_H(T) = |R_H(T)|/\rho(T)$ derived from these mea-

surements is plotted in Fig. 4. The respective values at 290 K are $39 \text{ cm}^2/\text{V s}$ and $1.8 \text{ cm}^2/\text{V s}$, and in both samples a negative slope is seen at room temperature, roughly following a $T^{-3/2}$ law expected from acoustic phonon scattering,¹⁰ indicating that this should be the dominant scattering mechanism at high temperatures.

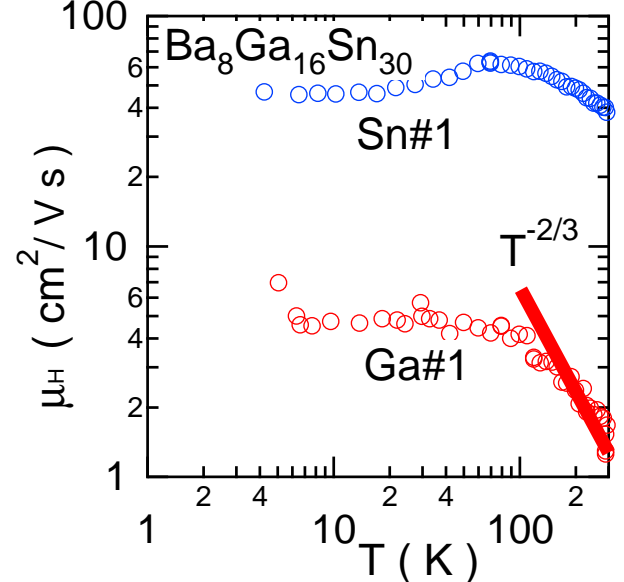


FIG. 4: (color online) Temperature dependence of the Hall mobility μ_H of $\text{Ba}_8\text{Ga}_{16}\text{Sn}_{30}$ crystals grown from Sn and Ga flux.

IV. DISCUSSION

The principle of operation of a thermoelectric cooling device requires a pair of materials, one n-type and one p-type, coupled electrically in series and thermally in parallel.¹¹ The device's performance optimization involves not only the properties of each individual branch, but a combined optimization of the thermoelectric pair. Thus, an important goal of research in this area is to not only find good thermoelectric materials of both carrier types, but also find materials that may be fine-tuned with respect to their figure of merit $ZT = S^2T/\rho\kappa$. Our experiments show that $\text{Ba}_8\text{Ga}_{16}\text{Sn}_{30}$ samples may be a candidate to fulfill most of these requirements.

The existence of n-type and p-type samples has already been observed in sintered samples with nominal compositions $\text{Ba}_8\text{Ga}_{16+x}\text{Sn}_{30-x}$.⁸ It was reported that a gradual decrease of n-type carriers for $-3 < x < -2$ is followed by a gradual increase of p-type carriers for $-1 < x < +2$, with a possible "quasi-insulating" region around $x = -1.5$. Our results clearly show that the flux grown crystals are strikingly more sensitive in terms of sample composition, such that off-stoichiometries of $x = \pm 0.1$ from the ideal value are enough to cause the drastic change.

If we can understand the reasons behind the observed differences in carriers and transport properties, we may be able to control these through the growth parameters and/or through post growth thermal treatment. The first issue is whether the observed differences are indeed primarily associated with stoichiometry. Our experimental data give good evidence that there is in fact a correlation with the Ga-Sn proportion, such that the transport properties can be directly related to the ionic doping level.

But the transport properties may not be directly related only to differences in stoichiometry. The next logical step is to account for differences in the distribution of Ga-Sn atoms throughout the cage structure. Contrary to the Ga-Ge clathrates where, due to size similarity of these two atoms, they show mostly random distribution throughout all three crystallographic sites of the type-I clathrate structure (although there are some indications of possible preferential occupations)^{4,12,13} in $\text{Ba}_8\text{Ga}_{16}\text{Sn}_{30}$ the size difference between Ga and Sn ions is large enough that there is a clear preferential occupation of at least three of their four different sites in the type-VIII clathrate structure. Assuming that random occupation of a given site implies in a proportion close to $\text{Ga}_{16}\text{Sn}_{30}$ in that site, our single crystal XRD refinement on the Sn#2 crystal revealed that Sn tends to favor the X(1) site ($\text{Ga}_{8.5}\text{Sn}_{37.5}$) and X(2) site ($\text{Ga}_{7.3}\text{Sn}_{38.7}$) while Ga tends to occupy the X(4) site ($\text{Ga}_{35.3}\text{Sn}_{10.7}$) which has the shortest bond distances between neighbors, and the X(3) site remains more randomly occupied by both atoms ($\text{Ga}_{14.4}\text{Sn}_{31.6}$). We performed a preliminary comparative investigation of the Sn#2 crystal before and after annealing for one week at 480 °C, which showed only a 12% decrease in its thermopower above room temperature, so that either the annealing condition was ineffective in significantly rearranging the as grown Ga-Sn distribution, or the differences in distribution may be indeed secondary with respect to thermoelectric properties, in comparison to composition differences.

V. CONCLUSION

Single crystals of $\text{Ba}_8\text{Ga}_{16}\text{Sn}_{30}$ grown from Sn flux and Ga flux have shown significantly different charge carrier densities and transport properties, which we could correlate to the relative Ga-Sn content in the crystals. The crossover between n-type and p-type carriers occurs within a very narrow range around the ideal 8:16:30 stoichiometry, in agreement with charge-balance principles and contrary to previously reported preliminary studies on sintered polycrystals. Such characteristics point to the possibility of tuning the charge carrier nature and density, as well as the transport properties, through the sample preparation process and possibly through post growth annealings, a desirable feature in any material intended for thermoelectric applications.

To our satisfaction, almost at the same time we were submitting this manuscript the research group from Dresden published two excellent works^{14,15} describing how their polycrystalline $\text{Eu}_8\text{Ga}_{16}\text{Ge}_{30}$ samples can be tuned with respect to composition, carrier concentration and thermoelectric properties, although in their case only n-type samples were found. Their results also challenge the current “tunneling” models for glass-like thermal conductivity (which we mentioned in the introduction section) attributing this low-temperature behavior to phonon-charge-carrier scattering instead.

Acknowledgments

We thank Y. Shibata for the electron-probe microanalysis. This work was financially supported by the COE Research (CE13CE2002) and the priority area “Skutterudite” (No. 15072205) through Grants-in-Aid from MEXT, Japan. D.H. is also supported by National Science Foundation of China (No.50471008).

¹ G. A. Slack, in *CRC Handbook of Thermoelectrics* (Chemical Rubber, Boca Raton, FL, 1995), chap. 34, p. 407.

² J. L. Cohn, G. S. Nolas, V. Fessatidis, T. H. Metcalf, and G. A. Slack, *Phys. Rev. Lett.* **82**, 799 (1999).

³ B. C. Sales, B. C. Chakoumakos, R. Jin, J. R. Thompson, and D. Mandrus, *Phys. Rev. B* **63**, 245113 (2001).

⁴ B. C. Chakoumakos, B. C. Sales, and D. G. Mandrus, *J. Alloys. Comp.* **322**, 127 (2001).

⁵ V. Keppens, M. A. McGuire, A. Teklu, C. Laermans, B. C. Sales, D. Mandrus, and B. C. Chakoumakos, *Physica B* **316-317**, 95 (2002).

⁶ I. Zerec, V. Keppens, M. A. McGuire, D. Mandrus, B. C. Sales, and P. Thalmeier, *Phys. Rev. Lett.* **92**, 185502 (2004).

⁷ D. Huo, T. Sakata, T. Sasakawa, M. A. Avila, M. Tsubota, F. Iga, H. Fukuoka, S. Yamanaka, S. Aoyagi, and T. Takabatake, *Phys. Rev. B* **71**, 075113 (2005).

⁸ T. Kurinaga, Y. Nagamoto, S. Ido, H. Hayase, and T. Koyanagi, *Thermoelectric Conversion Symp. 2000 Proc.*, Tokyo, Japan pp. 84-85 (2000).

⁹ D. R. Lovett, *Semimetals and Narrow-BandGap Semiconductors* (Pion Limited, London, 1977).

¹⁰ K. Seeger, *Semiconductors physics: an introduction* (Springer-Verlag, 1985).

¹¹ G. S. Nolas, J. Sharp, and H. J. Goldsmid, *Thermoelectrics - Basic Principles and New Materials Developments* (Springer, New York, 2001).

¹² B. C. Chakoumakos, B. C. Sales, D. G. Mandrus, and G. S. Nolas, *J. Alloys. Comp.* **296**, 80 (2000).

¹³ Y. Zhang, P. L. Lee, G. S. Nolas, and A. P. Wilkinson, *Appl. Phys. Lett.* **80**, 2931 (2002).

¹⁴ V. Pacheco, A. Bentien, W. Carrillo-Cabrera, S. Paschen, F. Steglich, and Y. Grin, *Phys. Rev. B* **71**, 165205 (2005).

¹⁵ A. Bentien, V. Pacheco, S. Paschen, Y. Grin, and F. Steglich, *Phys. Rev. B* **71**, 165206 (2005).